

CONTROL STRATEGY FOR A NON-HYBRID HYDROSTATIC TRANSMISSION CONSTRUCTION VEHICLE BASED ON POWER FOLLOWER

Haoyu YUAN¹, Jixin WANG², Shaofeng DU³, Yunwu HAN^{4*}, Jindong WANG⁵

¹*School of Mechanical and Aerospace Engineering, Jilin University, Changchun, China*

²*Chongqing Research Institute, Jilin University, Chongqing, China*

^{3,5}*State Key Laboratory of Smart Manufacturing for Special Vehicles and Transmission System, Baotou, China*

⁴*School of Intelligent Transportation, Jiangsu Vocational College of Electronics and Information, Huai'an, China*

Submitted 17 February 2020; resubmitted 23 October 2020, 12 December 2020; accepted 24 April 2021

Abstract. To achieve energy-saving control of non-hybrid Hydrostatic Transmission Construction Vehicles (HST-CVs) with traditional closed-loop Hydrostatic Transmission (HST) for both propulsion and working systems, this paper presents a control strategy for non-hybrid HST-CVs by referring to the power follower method of the hybrid Energy Management Strategy (EMS). Through the implementation of the presented control strategy by coordinated control of the engine speed and hydraulic pump displacement, the engine can be controlled to operate at the pre-set low Brake Specific Fuel Consumption (BSFC) area, similar to that of the hybrid vehicles adopting a power follower control strategy but without the additional installation of accumulators in the hydraulic system. The effect of the control strategy is verified via experimental tests and MATLAB/SIMULINK-AMESIM COLlaborative SIMulation (COSIM). The simulation results show that the proposed control strategy can achieve the expected control target under both highway and off-road conditions.

Keywords: hydrostatic transmission, control strategy, construction vehicle, energy-saving control, power follower, concrete mixer truck.

Notations

Abbreviations:

BSFC – brake-specific fuel consumption;
CAN – controller area network;
COSIM – collaborative simulation;
CV – construction vehicle;
DP – dynamic programming;
ECMS – equivalent consumption minimization strategy;
ECU – engine controller unit;
EDC – electronic displacement control;
EMS – energy management strategy;
HHV – hydraulic hybrid vehicle;
HST – hydrostatic transmission;
HST-CV – HST construction vehicle;
ICE – internal combustion engine;
Min BSFC Line – minimum BSFC line;
MPC – model predictive control;
NFPE – non-feedback proportional electrical;

OOL – optimal operating line;
PID – proportional–integral–derivative;
SDP – stochastic DP;
VCU – vehicle controller unit.

Variables and functions:

G_D – gear of propulsion direction;
 G_M – gear of propulsion motor displacement;
 G_T – gear of transmission;
 G_W – gear of working device speed;
 i_A – total reduction ratio of the drive bridge;
 i_R – reduction ratio of the working device reducer;
 i_T – reduction ratio of transmission;
 $k_{n,E \text{ lim}}$ – change rate limit value of the engine speed [rpm/s];
 $k_{Q,PPadj}$ – adjustment coefficient of the flow rate requirement of the propulsion pump;
 $k_{V,P \text{ lim}}$ – change rate limit value of the variable pump displacement [mL/r·s];

*Corresponding author. E-mail: 917946826@qq.com

$k_{\eta,PPt}$ – total efficiency coefficient of the propulsion pump;
 $k_{\eta,PPv}$ – volume efficiency coefficient of the propulsion pump;
 $k_{\eta,WPt}$ – total efficiency coefficient of the working pump;
 $k_{\eta,W Pv}$ – volume efficiency coefficient of the working pump;
 M_{PP} – input torque of the propulsion pump [N·m];
 n_E – engine speed [rpm];
 n_{Ecmd} – command value of the engine speed [rpm];
 n_{Ereq} – engine speed requirement [rpm];
 n_M – hydraulic motor speed [rpm];
 n_{PM} – propulsion motor speed [rpm];
 n_W – working device speed [rpm];
 n_{WM} – working motor speed [rpm];
 P_a – position of accelerator pedal [%];
 P_P – input power of the hydraulic pump [kW];
 P_{PH} – pressure of the propulsion system at high-pressure circuit [bar];
 P_{PL} – pressure of the propulsion system at low-pressure circuit [bar];
 P_{Preq} – power requirement of the propulsion system [kW];
 P_{req} – overall power requirement of HST-CV [kW];
 P_{Wreq} – power requirement of the working system [kW];
 P_{WH} – pressure of the working system at high-pressure circuit [bar];
 P_{WL} – pressure of the working system at low-pressure circuit [bar];
 Q_P – output flow rate of the hydraulic pump [L/min];
 Q_{PP} – output flow rate of the propulsion pump [L/min];
 Q_{PPadj} – adjusted flow rate requirement of the propulsion pump [L/min];
 Q_{PPreq} – flow rate requirement of the propulsion pump [L/min];
 Q_{WP} – output flow rate of the working pump [L/min];
 Q_{WPreq} – flow rate requirement of the working pump [L/min];
 r_{tire} – effective rolling radius of the tire [m];
 Δt – duration of one time step;
 v – vehicle speed [km/h];
 V_{PM} – propulsion motor displacement [mL/r];
 V_M – displacement of the hydraulic motor [mL/r];
 V_{PP} – propulsion pump displacement [mL/r];
 V_{PPcmd} – command value of the propulsion pump displacement [mL/r];
 V_{PPreq} – displacement requirement of the propulsion pump [mL/r];
 V_{WM} – working motor displacement [mL/r];
 V_{WP} – working pump displacement [mL/r];
 V_{WPreq} – displacement requirement of the working pump [mL/r];
 V_{WPcmd} – command value of the working pump displacement [mL/r];

Δp_{min} – pressure limit valve of the hydraulic pump inlet and outlet [bar];
 Δp_{PP} – pressure difference between the propulsion pump inlet and outlet [bar];
 Δp_{WP} – pressure difference between the working pump inlet and outlet [bar];
 η_{Mv} – volume efficiency of the hydraulic motor;
 η_{PMv} – volume efficiency of the propulsion motor;
 η_{PPm} – mechanical efficiency of the propulsion pump;
 η_{PPt} – total efficiency of the propulsion pump;
 η_{PPv} – volume efficiency of the propulsion pump;
 η_{Pt} – total efficiency of the hydraulic pump;
 η_{WMv} – volume efficiency of the working motor;
 η_{WPt} – total efficiency of the working pump;
 η_{WPv} – volume efficiency of the working pump.

Introduction

CV is a type of wheel drive vehicle for specific construction functions, typically including a wheel loader, scraper and concrete mixer truck. Compared with highway vehicles, the CV needs to operate the working device while driving, thus resulting in additional operating loads. With increasingly serious energy shortage and environmental pollution, more attention has been paid to ways of increasing the energy efficiency and achieving emission reduction of CVs as a type of vehicle with high energy consumption (Li *et al.* 2016). HST, owing to its advantages of high power density, step-less variable speed characteristic and high traction at low speed, has been widely used in CVs, agricultural machineries and other off-road vehicles (Backé 1993; Rydberg 1998).

Generally, a basic HST system contains a prime mover (typically a diesel engine), a variable displacement pump, a fixed or variable displacement motor and other hydraulic and electronic control components. The output speed of HST is controlled by regulating the rotational speed of the diesel engine and controlling displacements of the pump and motor (Wu *et al.* 2004). Recently, studies on HST control have mainly focused on the energy efficiency and the control performance. Nawrocka and Kwaśniewski (2008) applied the predictive neural network controller to control the rotational speed of the hydraulic engine HST. Aschemann *et al.* (2009) presented a nonlinear trajectory control scheme for drive chains based on HST, which showed an excellent control performance in simulation results. Sun and Aschemann (2013) proposed a sliding-mode approach with disturbance compensation for hydrostatic drive train tracking control, which obtained high tracking performance and robust stability of the closed-loop system. Zips *et al.* (2019) developed and applied an optimization-based control concept for real-time application on a commercial electronic control unit for HST of a wheel loader. The overall efficiency is maximized according to the evaluation results on a test track. Rydberg (1998)

pointed out that an attractive area for further development will be to fully integrate the engine in the drive train control system in a form that enables the vehicle to operate with optimum fuel consumption depending on the power required, but related studies are relatively scarce. Zhao *et al.* (2018) proposed a control strategy of the variable hydraulic pump according to the external characteristic curve of the engine, which enables the engine to work on 90% characteristic curve (traditional best fuel consumption curve) by regulating the displacement of the variable hydraulic pump to achieve the best fuel consumption. However, the strategy is still preliminary.

Compared with conventional non-hybrid HST vehicles, in series HHVs, given the existence of the accumulator, a constant pressure system is formed with the hydraulic pump and motor, transforming the pump and motor into independent control components. Because there is no direct coupling between the engine speed and vehicle speed, the engine can be operated to maximize fuel efficiency and minimize emissions. This characteristic makes series HHVs more flexible to control (Johri, Filipi 2014; Kim, Filipi 2007). Researchers have conducted numerous studies on series HHV's control strategies to reduce fuel consumption and exhaust emissions and improve vehicles' fuel economy performance. Kim and Filipi (2007) proposed power management for a simulation-based series HHVs based on the thermostatic state-of-charge approach. The fuel economy predictions indicated improvements exceeding 50% under urban driving conditions. Molla (2010) evaluated three hybrid power management strategies: a rule-based strategy, a globally optimal (drive cycle optimal) using DP algorithm and instantaneous optimization (ECMS) strategy based on an overall model of a series HHV independent wheel drive system. Considering the sensitivity of EMSs with respect to variations in drive cycle and system parameters, Deppen *et al.* (2015) presented three strategies of the series HHV's powertrain (rule-based, SDP and MPC) and experimentally validated these using a hardware-in-the-loop system. Hung *et al.* (2016) applied the DP methodology to derive the optimal power-splitting factor for the hybrid system for preselected driving schedules, and the results are used to improve rule-based control strategies, achieving further improvement in fuel economy.

Although the above control strategies can effectively achieve the energy-saving control in series HHVs, it is inapplicable to the HST-CV, which uses a traditional non-hybrid closed-loop HST system for both the propulsion and working systems. This condition is attributed to the lack of accumulator in the traditional closed-loop HST system and the establishment of the coupling relationship between hydraulic pumps and motors by the flow rate of the hydraulic system. The flow rate depends on the displacement of hydraulic pump and engine speed, whose changes will result in variations in the flow rate and speed

of hydraulic motor. Thus, the control of the ICE operating point cannot be implemented in the traditional non-hybrid closed-loop HST system. To overcome this limitation, this paper considers the flow rate of HST-CV propulsion/working system as the control target. By coordinated control of the engine speed and hydraulic pump displacement, the decoupling between the engine speed and flow rate of the hydraulic system can be achieved, and the engine speed can be controlled at the expected range. On this basis, referring to the power follower control strategy in the EMS of hybrid vehicles (Kim *et al.* 2014; Shabbir, Evangelou 2016), this paper proposes a control strategy for the non-hybrid HST-CV based on power follower. The proposed control strategy can achieve energy-saving control effects similar to the power follower control strategy of hybrid vehicles through the coordinated control of the engine speed and hydraulic pump displacement without modifying the basic structure of the HST-CV hydraulic system (without installing additional accumulators in the hydraulic system). This allows the engine to operate at the lower BSFC area to improve the HST-CV fuel economy performance. The feasibility and effect of the control strategy are verified by the load data capturing experiment and the MATLAB/SIMULINK–AMESIM COSIM platform.

This paper is organized as follows. Section 1 introduces the configuration of HST-CV basic vehicle. Section 2 presents the control strategy design for the non-hybrid HST-CV based on power follower. Section 3 establishes the COSIM platform and discusses the simulation results. Finally, the conclusions are summarized.

1. Configuration of HST-CV basic vehicle

The control strategy proposed in this paper considers a type of 1.5 m³ concrete mixer truck as the HST-CV basic vehicle. This type of CV uses the HST instead of a traditional mechanical transmission to transfer power from the engine to the propulsion and mix working system. Figure 1 shows the basic structural principle of HST-CV basic vehicle.

As shown in Figure 1, the driveline of HST-CV basic vehicle consists of the following structural components: engine, propulsion pump, working pump, propulsion motor, working motor, working device, transmission box and differential. Among these components, both the propulsion pump and working pump are plunger variable pumps, both of them are connecting to the engine in series and each forming a closed-loop HST system with the propulsion and working motors. The control system of HST-CV consists of the VCU and ECU, both running through a CAN bus to communicate. VCU also controls the displacement of propulsion pump, working pump and propulsion motor.

Table 1 shows the main parameters of the HST-CV basic vehicle.

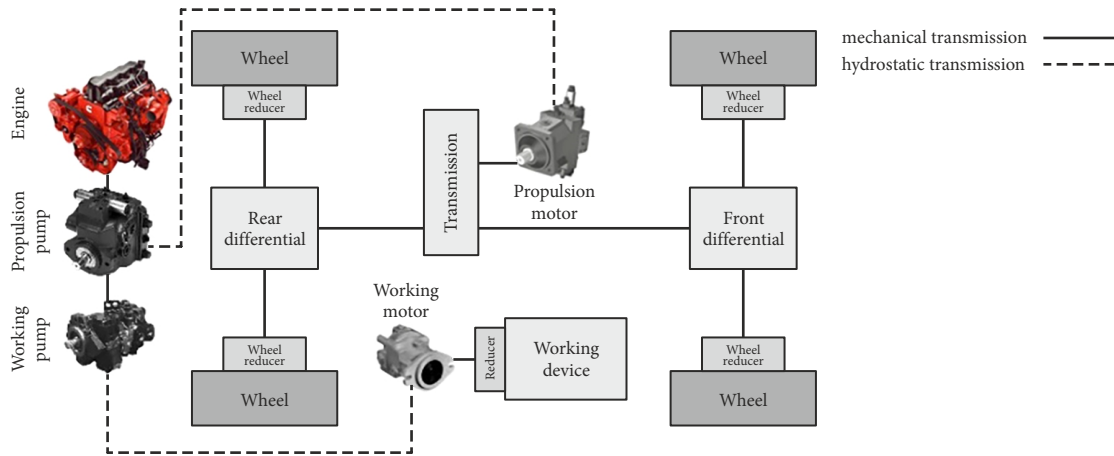


Figure 1. Structural principle of HST-CV basic vehicle

Table 1. HST-CV basic vehicle parameters

	Parameter	Value
Vehicle	Curb weight	4000 kg
	Full weight	8000 kg
	Maximum speed	30 km/h
	Speed of working device	5, 10, 15 rpm
Engine	Rated power	38 kW
	Rated speed	2500 rpm
	Maximum torque	165 N·m
Propulsion system	Pump type	plunger variable pump (EDC)
	Pump displacement	0...53 mL/r
	Motor type	plunger variable motor (EDC)
	Motor displacement	40 mL/r (low gear); 80 mL/r (high gear)
	Transmission reduction ratio	1:4.341 (off-road gear); 1:0.84 (highway gear)
	Drive bridge reduction ratio	1:12.158
	Tire effective rolling radius	0.4145 m
Working system	Pump type	plunger variable pump (EDC)
	Pump displacement	0...46 mL/r
	Motor type	gear motor
	Motor displacement	35 mL/r
	Reduction ratio of working device reducer	1:53

2. Control strategy

As mentioned above, the control strategy based on power follower for HST-CV proposed in this paper considers the flow rate of HST system as the control target. Through implementation of the coordinated control of the engine speed and hydraulic pump displacement, decoupling can be achieved between the hydraulic motor and engine speeds, similar to the series hydraulic hybrid powertrain system. Then, the control of the ICE operating point, which based on the power follower control strategy, can be implemented in HST-CV to achieve the energy-saving control.

To achieve the above control objectives, the following problems need to be discussed: how to transform the

driver's operation into the required flow rate control target, calculate the overall power requirement of HST-CV, plan the control target of the ICE operating point, and achieve coordinated control between the engine speed and hydraulic pump displacement. In addition, considering the possible engine flameout under heavy load conditions, such as slope climbing or starting conditions, in the control strategy development process, it is necessary to design an adaptive control strategy for the propulsion system based on the pressure feedback. To reduce the difficulty of system designs and improve the real-time capability of the control strategy, in this paper, the control strategy structure is established by the layered control method.

2.1. Control strategy structure

Figure 2 shows the layered control strategy structure of the proposed control strategy.

In Figure 2, P_a refers to the position of accelerator pedal; G_T denotes the gear of transmission and corresponds to the off-road/highway gear; G_D represents the gear of propulsion direction corresponding to the forward/stop/backward propulsion direction of the vehicle; G_M specifies the gear of propulsion motor displacement; G_W stands for the gear of working device speed corresponding to the 1st/2nd/3rd gear of working speed; n_{Ecmd} corresponds to the control command valve of engine speed; V_{PPcmd} indicates the control command valve of propulsion pump displacement; V_{WPcmd} is the control command valve of working pump displacement; p_{PH} , p_{PL} , p_{WH} , p_{WL} are the pressures of the propulsion/working system at high/low-pressure circuits when operating in the forward direction.

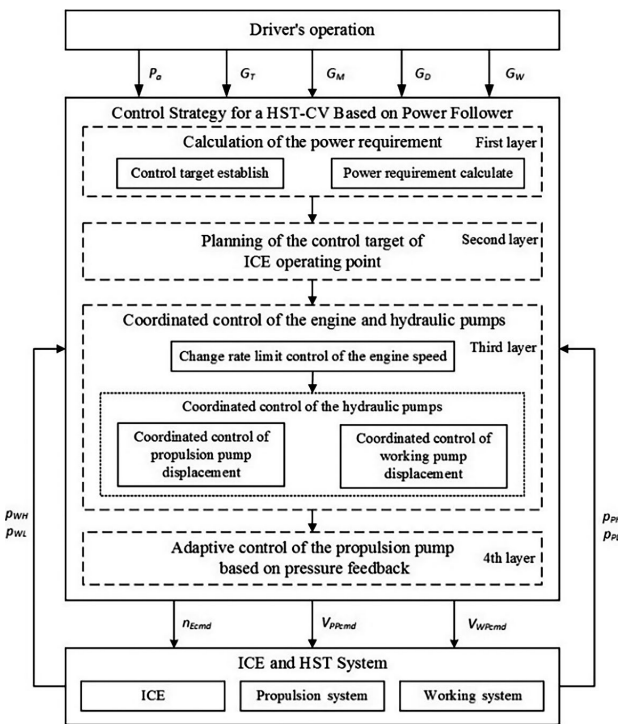


Figure 2. Layered control strategy structure

In the control strategy structure, according to the established corresponding relationship of the driver's operation and the flow rate control target, the first layer determines the flow rate control targets of the propulsion and working systems on the basis of the driver's operation. Based on this, the calculation of the overall power requirement of HST-CV is implemented by capturing the pressure of the propulsion/working systems. In the second layer, the control target of the ICE operating point is set up based on the overall power requirement of HST-CV. The specific control strategy structure of the first and second layers is shown in Figure 3.

Notably, the control target of the ICE operating point is not fixed and can be adjusted according to the driving requirements, operating environment, emissions, and/or economic operation requirements.

In the third layer, according to the ICE operating point (engine speed) control requirement obtained from the second layer, combined with the flow control requirements of the propulsion and the working systems determined in the first layer, the control of the engine and hydraulic pump is implemented through the change rate limit control of the engine speed and the coordinated control of the hydraulic pump displacement, respectively. At the same time, considering the possible engine flameout under heavy load conditions, the pressure of the HST system is used as the feedback in the fourth layer to adjust the displacement requirement of the propulsion pump in real time to further implement the adaptive control of propulsion pump displacement. The specific control strategy structure of the third and fourth layers is shown in Figure 4.

2.2. Flow rate control target

For the HST-CV, P_a , G_T , G_M , G_D and G_W reflect the driver's requirements of the vehicle speed, propulsion direction and working device speed. To implement the control of the flow rate of the propulsion and working systems, the corresponding relationship between the driver's operation and flow rate control target must be established.

For the propulsion system of the HST-CV, the vehicle speed can be expressed as follows:

$$v = \frac{3 \cdot \pi \cdot r_{tire} \cdot n_{PM}}{25 \cdot i_T \cdot i_A} \tag{1}$$

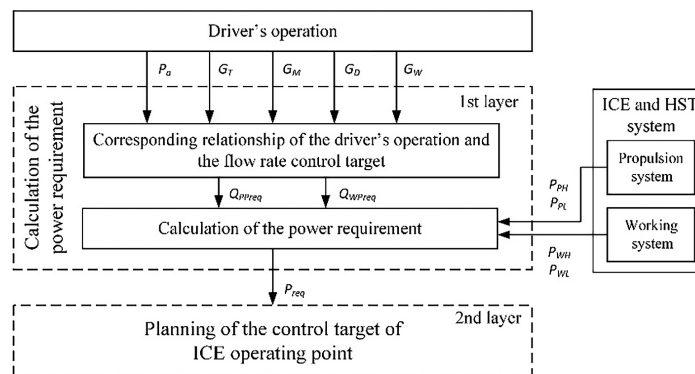


Figure 3. Control strategy structure of the first and second layers

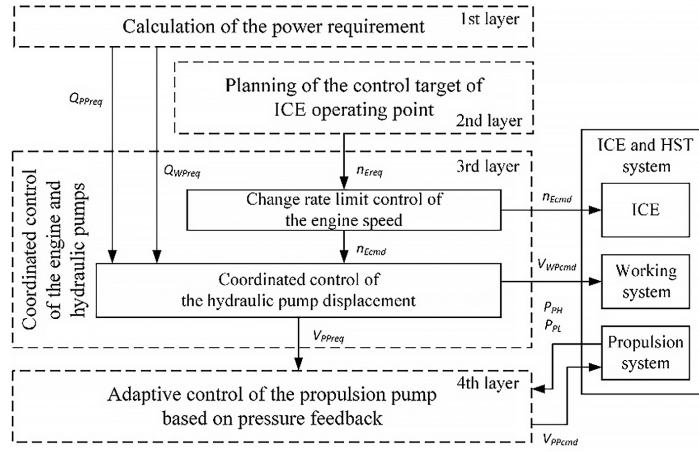


Figure 4. Control strategy structure of the third and fourth layers

Similarly, the speed of the HST-CV working device can be expressed as follows:

$$n_W = \frac{n_{WM}}{i_R}. \quad (2)$$

Meanwhile, the speed of hydraulic motor can be expressed by the following (Korn 1969):

$$n_M = \frac{1000 \cdot Q_P \cdot \eta_{Mv}}{V_M}. \quad (3)$$

Then, for the propulsion system of the HST-CV, according to Equations (1) and (3), v can be expressed as follows:

$$v = \frac{120 \cdot \pi \cdot r_{tire} \cdot Q_{PP} \cdot \eta_{PMv}}{i_T \cdot i_A \cdot V_{PM}}. \quad (4)$$

As shown in Equation (4), both i_T and V_{PM} are determined, and in the condition of neglect η_{PMv} , v is directly dependent on Q_{PP} . Therefore, this paper considers Q_{PP} as the corresponding parameter for the flow rate control target of the propulsion system and proposes Q_{PPreq} as the requirement for Q_{PP} , which is used in the control process.

For η_{PMv} , as shown in Table 1, the propulsion motor of the basic vehicle is a plunger variable motor; the volume efficiency of the motor is correlated with its speed, displacement, and system pressure, and the relationship between the volume efficiency and correlated parameters is complicated (Daikin-Sauer-Danfoss 2020). Therefore, to simplify the process of flow rate control target establishment, η_{PMv} is temporarily simplified to a constant value of 1. This value clearly deviates from the actual η_{PMv} during the HST-CV operation, which will cause the actual vehicle speed to be less than the expected vehicle speed. In this paper, the difference between the expected and actual vehicle speed is adjusted by $k_{\eta_{PPv}}$ (Section 2.5.2).

As shown in Table 1, the maximum v of the HST-CV basic vehicle is 30 km/h, which corresponds to the driver's operation as follows: P_a is 100%, G_T is the highway gear, and its reduction ratio is 0.84. G_M is the low-displacement gear, the propulsion pump displacement is 40 mL/r, and G_D is the forward gear. At this point, Q_{PPreq} should be rounded to 80 L/min.

Accordingly, P_a and Q_{PPreq} can form the following linear correspondence, as shown in Table 2.

Similar to the propulsion system, the working device speed can be expressed as follows:

$$n_W = \frac{1000 \cdot Q_{WP} \cdot \eta_{WMv}}{i_R \cdot V_{WM}}. \quad (5)$$

As presented in Equation (5), both i_R and V_{WM} are determined, and in the condition of neglect η_{WMv} , n_W is directly dependent on Q_{WP} . Therefore, this paper considers Q_{WP} as the corresponding parameter for the flow rate control target of the working system and proposes Q_{WPreq} as the requirement for Q_{WP} , which is used in the control process.

Similar to the propulsion system, in the process of flow rate control target establishment of the working system, η_{WMv} is temporarily simplified to a constant value of 1. The resulting difference between the expected and actual working device speed is adjusted by $k_{\eta_{WPv}}$ (Section 2.5.2).

As shown in Table 1, n_W of the HST-CV basic vehicle is 5, 10, 15 rpm, corresponding to the 1st, 2nd, 3rd gear of G_W , respectively, and i_R is fixed at 1:53. Thus, Q_{WPreq} in the 1st, 2nd, 3rd gear of G_W should be 14.5, 29.2, 43.7 L/min, respectively.

Accordingly, G_W and Q_{WPreq} can form the following correspondence, as shown in Table 3.

2.3. Calculation of the power requirement

For the HST system, the input power of the hydraulic pump can be obtained from the following equation (Korn 1969):

$$P_p = \frac{Q_p \cdot \Delta p_p}{600 \cdot \eta_{pt}}. \quad (6)$$

Table 2. Corresponding relationship of the driver's operation and the flow rate control target of the propulsion system

Driver's operation	Valve	Flow rate control target	Valve
$P_a(t)$ [%]	0	$Q_{PPreq}(t)$ [L/min]	0
	100		80

Table 3. Corresponding relationship of the driver's operation and the flow rate control target of the working system

Driver's operation	Valve	Flow rate control target	Valve
$G_W(t)$ [-]	1	$Q_{WPreq}(t)$ [L/min]	14.5
	2		29.2
	3		43.7

According to Equation (6), P_p depends on Q_p and Δp_p while ignoring the influence of hydraulic pump efficiency.

Section 2.2 establishes the corresponding relationship between the driver's operation and flow rate control target. Thus, Q_{PPreq} and Q_{WPreq} can be obtained by P_a and G_W , respectively. At the same time, by using the pressure sensor to collect p_{PH} , p_{PL} , p_{WH} and p_{WL} , the pressure difference between the inlet and outlet of the propulsion and working pumps can be calculated. By substituting the above parameters in Equation (6), the current power requirement of the propulsion and working systems can be obtained, as shown in Equations (7) and (8), respectively:

$$P_{Preq}(t) = \frac{Q_{PPreq}(t) \cdot \Delta p_{PP}(t)}{600 \cdot \eta_{PPt}}; \quad (7)$$

$$P_{Wreq}(t) = \frac{Q_{WPreq}(t) \cdot \Delta p_{WP}(t)}{600 \cdot \eta_{WPt}}. \quad (8)$$

According to Equations (7) and (8), the overall power requirement of HST-CV can be obtained by following equation:

$$P_{req}(t) = P_{Preq}(t) + P_{Wreq}(t). \quad (9)$$

As shown in Table 1, for the HST-CV basic vehicle studied in this paper, the propulsion and working pumps are both plunger variable pumps. The total efficiency of pumps are correlated with both the speed and system pressure of the pump, and the relationship between the total efficiency and correlated parameters is complicated but is mainly within the range of 80...89% (Daikin-Sauer-Danfoss 2020). To reduce the complexity of the control strategy, in this paper, η_{PPt} and η_{WPt} in Equations (7) and (8), respectively, are unified as the total efficiency coefficient of the propulsion/working pumps ($k_{\eta,PPt}$, $k_{\eta,WPt}$), as shown in Equations (10) and (11), respectively. The value of $k_{\eta,PPt}$ and $k_{\eta,WPt}$ are constant and adjusted by the results of the real vehicle test to ensure the accuracy of the power requirement calculation.

$$P_{Preq}(t) = \frac{Q_{PPreq}(t) \cdot \Delta p_{PP}(t)}{600 \cdot k_{\eta,PPt}}; \quad (10)$$

$$P_{Wreq}(t) = \frac{Q_{WPreq}(t) \cdot \Delta p_{WP}(t)}{600 \cdot k_{\eta,WPt}}. \quad (11)$$

The simplification of η_{PPt} and η_{WPt} will result in a difference between the power requirement obtained by the above equations and the actual power consumption of the HST-CV during operation, which will cause the engine

operating point to deviate from the control target. Therefore, when determining the value of $k_{\eta,PPt}$ and $k_{\eta,WPt}$, it is necessary to refer to the actual range of the engine operating point to ensure that it is as close as possible to the control target.

In addition, considering that when the propulsion system and the working device of HST-CV are both in non-working condition, both Δp_{PP} and Δp_{WP} remain zero values. At this point, regardless of the operation of the driver, according to Equations (9)–(11), P_{req} will retain a zero value, and the driver's operation will remain unresponded to. To avoid this undesired situation, in this paper, the values of Δp_{PP} and Δp_{WP} are limited by the pressure limit valve of the hydraulic pump inlet and outlet, Δp_{min} , and when they are less than Δp_{min} , the calculation will be replaced by Δp_{min} . Then, Equations (10) and (11) can be respectively rewritten as follows:

$$P_{Preq}(t) = \begin{cases} \frac{Q_{PPreq}(t) \cdot \Delta p_{min}}{600 \cdot k_{\eta,PPt}}, & \Delta p_{PP}(t) < \Delta p_{min}; \\ \frac{Q_{PPreq}(t) \cdot \Delta p_{PP}(t)}{600 \cdot k_{\eta,PPt}}, & \Delta p_{PP}(t) > \Delta p_{min}; \end{cases} \quad (12)$$

$$P_{Wreq}(t) = \begin{cases} \frac{Q_{WPreq}(t) \cdot \Delta p_{min}}{600 \cdot k_{\eta,WPt}}, & \Delta p_{WP}(t) < \Delta p_{min}; \\ \frac{Q_{WPreq}(t) \cdot \Delta p_{WP}(t)}{600 \cdot k_{\eta,WPt}}, & \Delta p_{WP}(t) > \Delta p_{min}. \end{cases} \quad (13)$$

2.4. Planning of the control target of ICE operating point

In the EMS of hybrid vehicles, the control method based on the minimum BSFC line (Min BSFC Line) is widely adopted (Johri, Filipi 2014; Kim, Filipi 2007; Filipi, Kim 2010; Vu *et al.* 2014). Figure 5 shows the Min BSFC Line obtained by the engine BSFC map of the HST-CV basic vehicle studied in this paper. Note that because of the China Nacional Standard (GB20819-2014), for the engine of an HST-CV basic vehicle, the engine speed of 1800 rpm is used as part of the emission limit standard test. Therefore, the tuning of the speed area near 1800 rpm is mainly based on emission rather than fuel consumption, which makes the BSFC at 1800 rpm slightly higher than those at adjacent areas, resulting in the two lowest BSFC areas in the engine BSFC map of the HST-CV basic vehicle.

As depicted in Figure 5, if the control method based on the Min BSFC Line is adopted as the engine control method for HST-CV, the power ranging from 25 to 35 kW is the high-speed operating range of the engine, whereas in the majority power range from 5 to 20 kW, the engine operates in the middle or low-speed range from 800 to 1600 rpm.

In addition, for Q_{PP} , the following relationship with the engine speed is obtained (Korn, 1969):

$$Q_{PP} = \frac{V_{PP} \cdot n_E \cdot \eta_{PPv}}{1000}. \quad (14)$$

According to Equation (14), during the HST-CV operation, Q_{PP} depends on both n_E and V_{PP} . Thus, a low n_E will result in low Q_{PP} , which will further affect the vehicle speed and vehicle power performance.

For the above reasons, based on the Min BSFC Line shown in Figure 5, in this paper, the control target of ICE operating point is adjusted to form the ICE OOL, which is more suitable for the HST-CV, as shown in Figure 6. The main points of the ICE OOL are indicated by the letters A–G, the values of which are listed in Table 4.

As shown in Figure 6, compared with the Min BSFC Line, the ICE operating point with 10...20 kW power range is adjusted from the Min BSFC area of 220 g/kW·h to the sub-optimal BSFC area between 220...230 g/kW·h. Thus, in the majority of the power range from 15 to 35 kW, the engine will operate in the middle and high-speed range of over 1600 rpm, which can achieve the energy-saving control of the engine while ensuring the power performance of HST-CV. Meanwhile, the adjustment of the ICE operating point in the partial power range also makes the ICE OOL smoother and reduces the possibility of engine speed stepping in the control process.

Table 4. Values of the main ICE OOL points

Point	Engine speed [rpm]	Engine torque [N·m]	Power [kW]
A	800	59.69	5
B	1300	73.46	10
C	1500	84.26	15
D	2000	95.50	20
E	2100	113.69	15
F	2200	130.23	30
G	2300	145.33	35

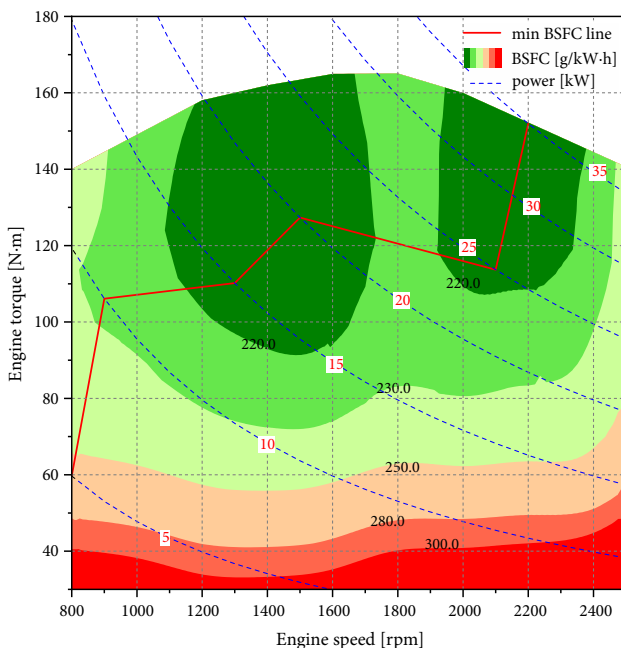


Figure 5. Min BSFC Line of HST-CV basic vehicle

To implement the control of the engine speed, this paper considers the engine speed requirement, n_{Ereq} , as the control variable for n_E . The corresponding relationship between n_{Ereq} and P_{req} can be derived from the ICE OOL (Figure 6), as shown in Figure 7. The values of points A–G, shown in Figure 7, are the same as those of the corresponding points in Figure 6 and Table 4.

2.5. Coordinated control of the engine and hydraulic pumps

Similar to Equation (14), for the output flow rate of the working pump, a relationship with n_E is shown in the following:

$$Q_{WP} = \frac{V_{WP} \cdot n_E \cdot \eta_{WPv}}{1000}. \quad (15)$$

According to Equations (14) and (15), to ensure that Q_{PP} and Q_{WP} will remain stable during the control of n_E and to implement the decoupling between the driving/working speed and engine speed, the coordinated control for n_E and V_{PP} , V_{WP} is necessary.

2.5.1. Change rate limit control of the engine speed

When the variable displacement pump is operating, to avoid the system pressure shock caused by the sudden change in displacement, a damping hole is added in the hydraulic proportional control loop of the pump to increase the response time of the hydraulic pump displacement from zero to maximum, or vice-versa (Daikin-Sauer-Danfoss 2020). Therefore, in the coordinated control of the engine speed and the variable pump displacement, the change rate of the engine speed during pump operation must be limited to adapt to the response time of the variable pump displacement.

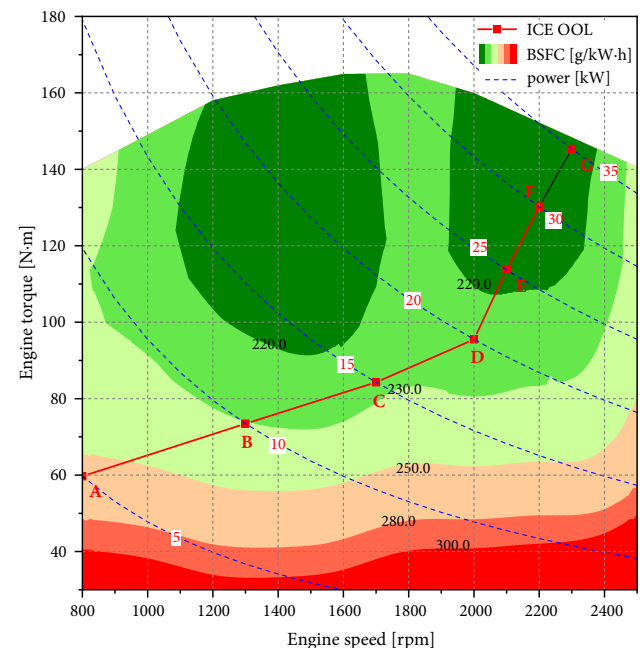


Figure 6. ICE OOL of HST-CV basic vehicle

In this paper, the change rate limit control of the engine speed is implemented by controlling the command value of the engine speed from the VCU. The specific control method is shown in following equation:

$$n_{Ecmd}(t) = \begin{cases} n_{Ereq}(t), & a_1; \\ n_{Ecmd}(t - \Delta t) \pm k_{n,Elim} \cdot \Delta t, & a_2, \end{cases} \quad (16)$$

where:

$$a_1 : |n_{Ereq}(t) - n_{Ecmd}(t - \Delta t)| < k_{n,Elim};$$

$$a_2 : |n_{Ereq}(t) - n_{Ecmd}(t - \Delta t)| > k_{n,Elim}.$$

In addition, the change rate limit of engine speed can effectively reduce the transient fuel consumption and emissions of the engine (Mishra, Saad 2017) and improve the economic performance of the HST-CV.

2.5.2. Coordinated control of the hydraulic pump displacement

According to Equation (14), the propulsion pump displacement can be expressed as follows:

$$V_{PP} = \frac{1000 \cdot Q_{PP}}{n_E \cdot \eta_{PPv}}. \quad (17)$$

In addition, to avoid the undesirable engine speed fluctuation caused by the vehicle's dynamic characteristics, this paper considers n_{Ecmd} instead of n_E as the control variable for V_{PP} . Similarly, Q_{PPreq} is used instead of Q_{PP} , and the volume efficiency coefficient of the propulsion pump, $k_{\eta,PPv}$, is used instead of η_{PPv} (similar to $k_{\eta,PPp}$, $k_{\eta,WPp}$, see Section 2.3). As a result, Equation (17) can be rewritten as follows:

$$V_{PPreq}(t) = \frac{1000 \cdot Q_{PPreq}(t)}{n_{Ecmd}(t) \cdot k_{\eta,PPv}}. \quad (18)$$

The adjustment to $k_{\eta,PPv}$ can actually be equivalent to the adjustment of the actual vehicle speed. When $k_{\eta,PPv}$ decreases, V_{PP} , Q_{PP} and v increase. The actual speed of the HST-CV in operation is related to many efficiency parameters, such as η_{PMv} and η_{PPv} . If a 3D table lookup or parameter estimation is used to determine the efficiency parameters, the control system will be overly complicated. Therefore, in this paper, the difference between the expected vehicle speed determined by P_a (Table 2) and the actual vehicle speed is adjusted by $k_{\eta,PPv}$ to bring them closer.

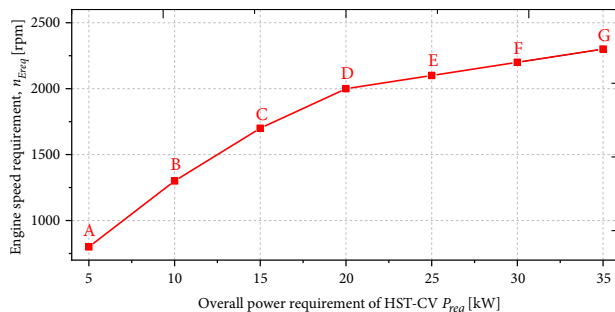


Figure 7. Corresponding relationship between the overall power requirement of HST-CV and the engine speed requirement

Equation (18) calculates for V_{PPreq} , where Q_{PPreq} can be obtained by P_a (Table 2); n_{Ecmd} is obtained by the ICE OOL (Figure 7) and adjusted by the change rate limit control of the engine speed.

Similar to the propulsion system, for the working system, the displacement requirement of the working pump can be expressed as follows:

$$V_{WPreq}(t) = \frac{1000 \cdot Q_{WPreq}(t)}{n_{Ecmd}(t) \cdot k_{\eta,WPv}}. \quad (19)$$

Similar to the propulsion system, the difference between the expected and actual working device speed is adjusted by $k_{\eta,WPv}$ to bring them closer.

At the same time, to decrease the pressure impact caused by the instantaneous change in hydraulic pump displacement, the change rate of the hydraulic pump displacement should be limited.

In this paper, the change rate limit control of the hydraulic pump displacement is implemented by controlling the command value of the hydraulic pump displacement from the VCU. The specific control method is shown in following equations:

$$V_{PPcmd}(t) = \begin{cases} V_{PPreq}(t), & a_1; \\ V_{PPcmd}(t - \Delta t) \pm k_{V,Plim} \cdot \Delta t, & a_2; \end{cases} \quad (20)$$

$$V_{WPcmd}(t) = \begin{cases} V_{WPreq}(t), & b_1; \\ V_{WPcmd}(t - \Delta t) \pm k_{V,Plim} \cdot \Delta t, & b_2, \end{cases} \quad (21)$$

where:

$$a_1 : |V_{PPreq}(t) - V_{PPcmd}(t - \Delta t)| < k_{V,Plim};$$

$$a_2 : |V_{PPreq}(t) - V_{PPcmd}(t - \Delta t)| > k_{V,Plim};$$

$$b_1 : |V_{WPreq}(t) - V_{WPcmd}(t - \Delta t)| < k_{V,Plim};$$

$$b_2 : |V_{WPreq}(t) - V_{WPcmd}(t - \Delta t)| > k_{V,Plim}.$$

For $k_{n,Elim}$ (see Section 2.5.1) and $k_{V,Plim}$, larger change rate limit values can make the engine and pumps operating more stable and also reduce the effects of the engine and pumps dynamic characteristics. However, compared with the lower $k_{n,Elim}/k_{V,Plim}$ (in this condition, the difference between the requirements and command values is smaller), the distribution of engine operating points will be more dispersed. The $k_{n,Elim}/k_{V,Plim}$ needs to be considered comprehensively in the actual process.

2.6. Adaptive control of the propulsion pump based on pressure feedback

During the operation of the HST-CV, the torque, which is the input torque of the propulsion pump, acts on the engine crankshaft from the propulsion system and can be expressed as follows (Korn 1969):

$$M_{PP} = \frac{V_{PP} \cdot \Delta p_{PP}}{20 \cdot \pi \cdot \eta_{PPm}}. \quad (22)$$

When the HST-CV is under heavy load conditions, such as slope climbing or starting conditions, Δp_{PP} will

rise sharply, and if V_{PP} is improperly controlled at this time, it may cause an engine flameout due to excessive M_{PP} .

To avoid the above undesirable situation, existing HST systems adopt control methods such as NFPE control or other similar NF-type control methods to react to system pressure, typically reducing the variable pump displacement with increasing pressure (Schumacher et al. 2016). Similarly, this paper proposes an adaptive control of the propulsion pump based on pressure feedback. However, because the displacement of the propulsion pump is indirectly obtained through the coordinated control based on the flow rate requirement of the propulsion pump, this paper introduces the adjustment coefficient of the flow rate requirement of the propulsion pump, $k_{Q,PPadj}$ and considers Δp_{PP} as the feedback signal to adjust Q_{PPreq} in real-time to reduce V_{PP} when Δp_{PP} rises sharply (Equation (18)), thus preventing the engine flameout due to excessive M_{PP} . Figure 8 shows the obtained method of $k_{Q,PPadj}$.

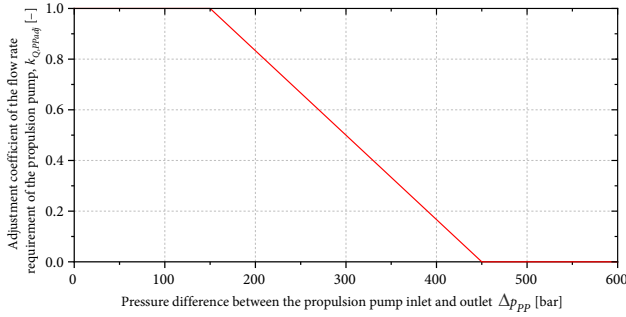


Figure 8. Obtained method for the adjustment coefficient of the flow rate requirement of the propulsion pump

The adjustment method for Q_{PPreq} is shown as follows:

$$Q_{PPadj}(t) = k_{Q,PPadj}(t) \cdot Q_{PPreq}(t). \quad (23)$$

At the same time, Equation (18) should be rewritten as follows:

$$V_{PPreq}(t) = \frac{1000 \cdot Q_{PPadj}(t)}{n_{Ecmd}(t) \cdot k_{\eta,PPV}}. \quad (24)$$

The overall diagram of the control loop of the proposed control strategy is shown in Figure 9.

3. Load data capturing experiment and simulation analysis

Because of the delay at the supplier's end and other factors, a prototype vehicle for testing the control strategy proposed in this paper has not yet been manufactured. Thus, to verify the effect of the control strategy for the non-hybrid HST-CV based on power follower, a MATLAB/Simulink-AMESIM COSIM platform is established in this paper. In addition, the driver's operation and pressure data of the propulsion/working systems when using the HST-CV under combined driving/working conditions are collected by the load data capturing experiment as the input of the COSIM platform to ensure the accuracy of the simulation results. Finally, the simulation results are analysed comprehensively.

3.1. Load data capturing experiment

In this paper, a type of 1.5 m³ concrete mixer truck with HST propulsion and mix working system is selected as the experimental vehicle for load data capturing, and its main performance parameters are the same as shown in Table 1.

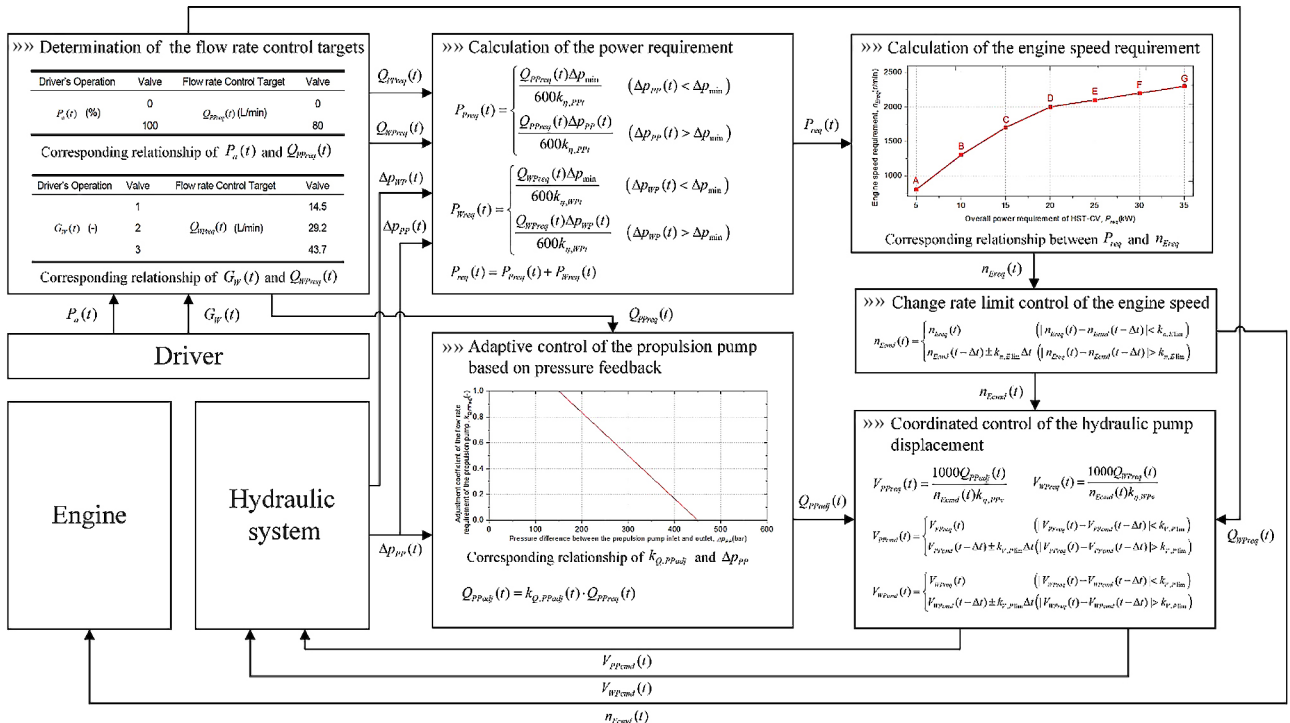


Figure 9. Diagram of the control loop of the proposed control strategy

To make the pressure data of the propulsion/working system cover more operating conditions, the load data capturing experiment is implemented in both the highway and off-road conditions. Figure 10 shows the experimental road conditions.

The highway condition, shown in Figure 10a, is a typical asphalt pavement. The off-road condition, shown in Figure 10b, is a typical off-road pavement in rural North China, which has compacted brown soil and a flat but rugged terrain, which is the same as the main off-road operating condition of the HST-CV basic vehicle. Because the experiment was conducted in winter, there was a small amount of snow on the off-road tracks.

Table 5 lists the load data capturing experiment scheme.

Figures 11 and 12 show the obtained driver’s operation and pressure data of the propulsion/working systems, respectively.

Figures 11 and 12 show that the pressure data of the working system under the off-road condition are similar to those for the highway condition, but the pressure fluctuation of the propulsion system under the off-road condition is much drastic than that under the high way condition. The variation trends of the pressure data of the propulsion/working system under the highway and off-road conditions are the same, and both correspond to the driver’s operation. Considering the pressure data of the propulsion/working system under the highway condition in Figure 11b as an example, the pressure peak of p_{PH} at 6...12 s corresponds to the starting condition of the vehicle. The two pressure fluctuations of p_{WH} at 26 and 47 s correspond to G_W shift from the 1st to 2nd gear and from the 2nd to 3rd gear, respectively. The pressure peak of p_{PL} at 67...71 s before the end of driving corresponds to the

pressure increase in the low-pressure circuit of the propulsion system caused by the driver’s braking operation. During driving, p_{WL} is constantly stable.

3.2. Simulation and analysis of results

Based on the driver’s operation and the pressure data from the load data capturing experiment. In this paper, the simulation model of the engine and the HST system of HST-CV is established by LMS® Imagine Lab AMESIM. Meanwhile, the simulation model of the control system is established by MATLAB/Simulink, and the control effect of the proposed control strategy will be verified by the MATLAB/Simulink–AMESIM COSIM platform consisting of both.

3.2.1. Simulation model of the engine and the HST system

Considering the influence of numerous nonlinear parameters in the engine and the HST system of HST-CV, it is difficult and time-consuming to establish the simulation model based on the mechanism analysis. Therefore, this paper adopts the LMS® Imagine Lab AMESIM software, which has a relatively complete model library of hydraulic and transmission system components. On the basis of the structural principle of the HST-CV basic vehicle shown in Figure 1, a simulation model of the engine and HST system of HST-CV is established, as shown in Figure 13. Because the pressure data of the propulsion/working system are selected as the load conditions of simulations, only the engine and the hydraulic pumps need to be modelled.

The parameter settings of the simulation model are the same as shown in Table 1.

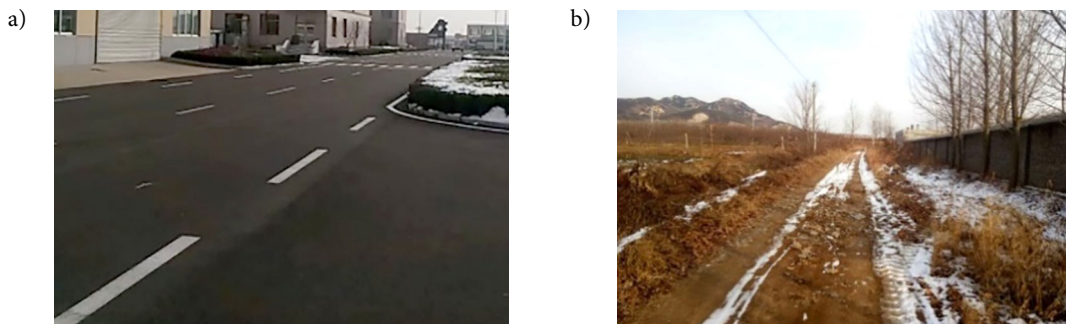


Figure 10. Experimental road conditions: a – highway condition; b – off-road condition

Table 5. Experimental scheme of the load data capturing experiment

Vehicle state before starting condition		Driver’s operation	Notes
Loading material	sand and stone dry material	»» shift the speed gear of working device to the 1st gear; »» start the vehicle;	»» the vehicle should be kept in a straight line while driving; »» the driver should step on the accelerator pedal to full opening and maintain while driving.
Gear of working device speed	gear 0	»» keep straight driving for about 75 m; »» shift the speed gear of working device to the 2nd gear;	
Gear of transmission	off-road gear	»» keep straight driving for about 75 m; »» shift the speed gear of working device to the 3rd gear;	
Displacement of propulsion pump	80 mL/r	»» keep straight driving for about 75 m; »» stop the vehicle.	

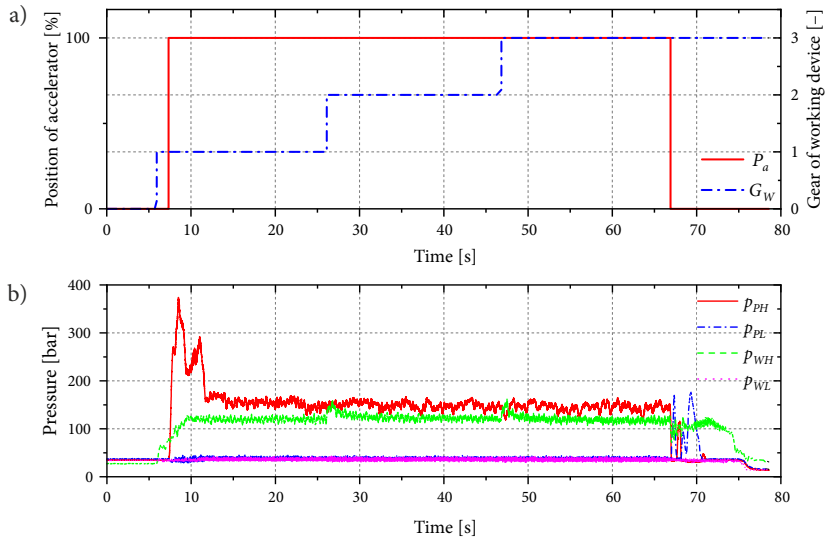


Figure 11. Captured data under the highway condition: a – driver’s operation; b – pressure data of the propulsion/working system

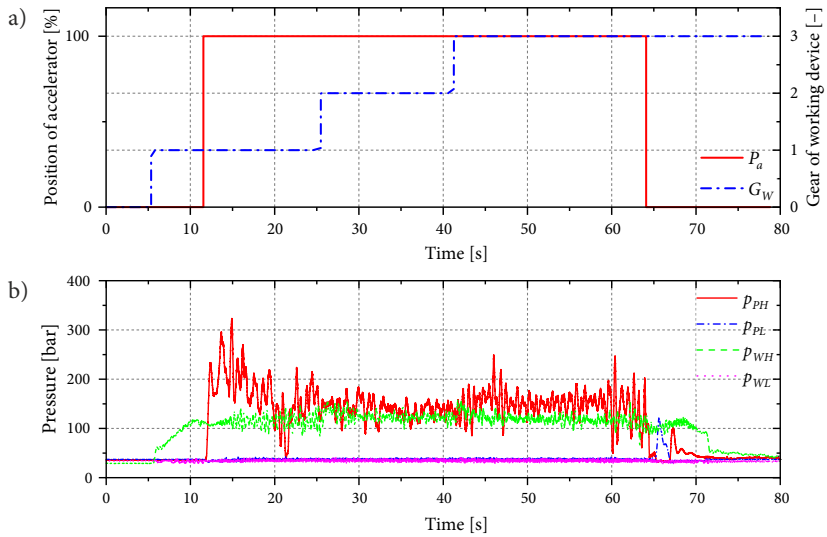


Figure 12. Captured data under the off-road condition: a – driver’s operation; b – pressure data of the propulsion/working system

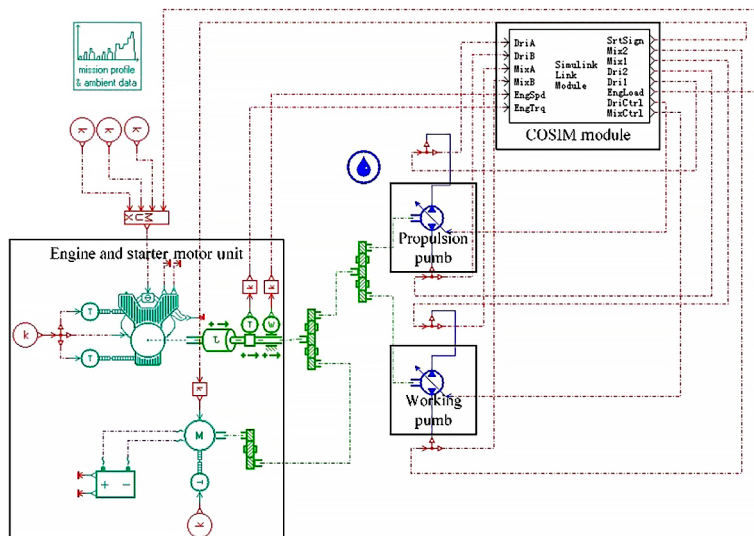


Figure 13. Simulation model of the engine and HST system of HST-CV

3.2.2. Simulation model of the control system

As shown in Figure 14, the overall simulation model of the control system of HST-CV includes the driver model, load model, ECU module, MATLAB/Simulink–AMESIM CO-SIM module, propulsion system control module, working system control module and engine control module.

Among them, the propulsion system control module, working system control module and engine control module were used for implementing the various control strategies described in Section 2. The COSIM module was used for implementing the data interaction between the MATLAB/Simulink-based control system simulation model and the AMESIM-based engine and the HST system simulation model. The driver and load models are based on the driver’s operation and pressure data of the propulsion/working system obtained from the load data capturing experiment as inputs to the COSIM platform. The ECU model adopts the PID method to adjust the load (value range: 0...1, dimensionless) of the engine model in AMESIM to realize the simulation of the full-range speed governing characteristic (7% governing rate) of the diesel engine.

3.2.3. Analysis of simulation results under the highway condition

The driver’s operation and pressure data of the propulsion/working system under the highway condition showed in Figure 11, are considered as the input of the COSIM platform. The simulation results are shown in Figure 15.

In Figure 15a, when the vehicle under the starting condition at 7...12 s, under the effect of the adaptive control of the propulsion pump based on pressure feedback, by adjusting the $k_{Q,PPadj}$ Q_{PPadj} produces a notable valley val-

ue, corresponding to the pressure peak of p_{PH} at 7...12 s in Figure 11b. Figures 15b and 15c also show that during the 7...12 s period, P_{req} , P_{Preq} and n_{Ecmd} remain stable, and no similar peak as p_{PH} occurs. Meanwhile, in Figure 15e, n_E is also stable, and no speed drop-off nor flameout results from the pressure peak of p_{PH} , which is consistent with the expected control target of the adaptive control of the propulsion pump based on pressure feedback.

In Figure 15b, except for the vehicle starting condition at 7...12 s, as p_{PH} and Q_{PPadj} are both stable (Figures 11b and 15a, respectively), P_{Preq} is stable in the vicinity of 15 kW. Although except for the pressure fluctuations during G_W gear shifting, p_{WH} under the highway condition remains stable (Figure 11b), but influences the step change of Q_{WPreq} (Figure 15a), P_{Wreq} also step changes. The value of Q_{req} is equal to the sum of P_{Preq} and P_{Wreq} , and it is stable during the simulation and maintained at the power range of 15...25 kW.

In Figure 15c, n_{Ecmd} which is obtained by the ICE OOL, is also stable in the middle and high-speed range of 1700...2200 rpm, which is consistent with the expected control target of the planning of the ICE operating point.

In Figure 15d, as P_{req} is lower before the vehicle is started, n_{Ecmd} is only maintained at idle speed. Therefore, a higher V_{WPcmd} is required to maintain the operating speed of the working device, resulting in the high-level platform of V_{WPcmd} before 7 s. Then, except for the influence of Q_{WPreq} step change, V_{WPcmd} remain stables. Under the coordinated control of the engine speed and hydraulic pump displacement, the variation trend of V_{WPcmd} is opposite to that of n_{Ecmd} . For V_{PPcmd} , which is influenced by the change rate limit control of the engine speed, n_{Ecmd} is difficult to increase to a high value within a very short time.

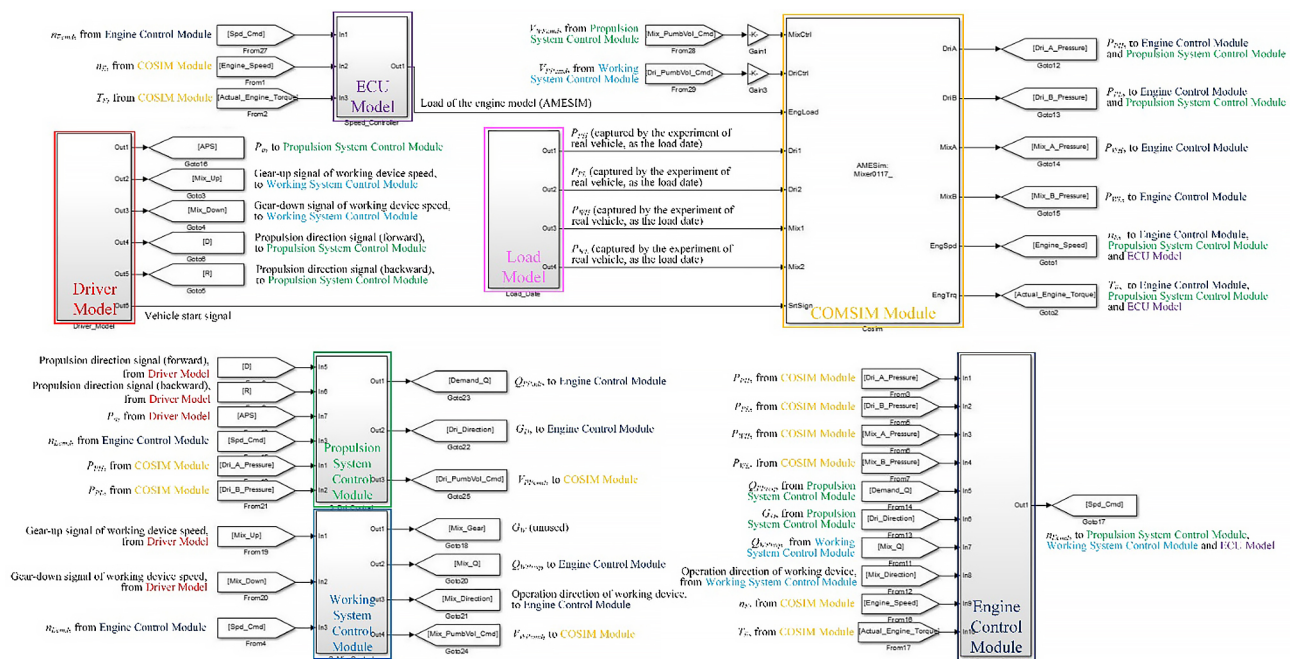


Figure 14. Simulation model of the control system of HST-CV

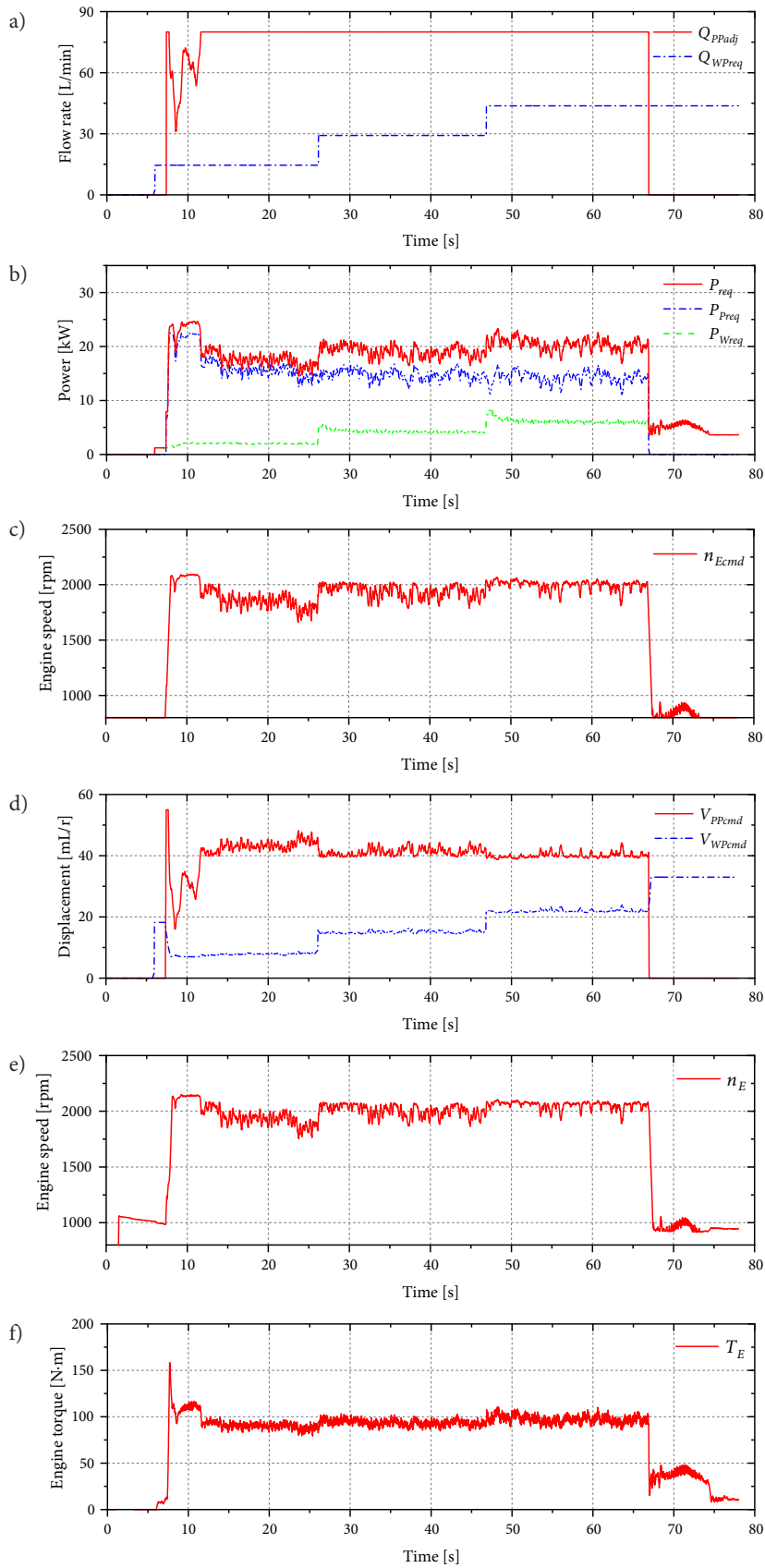


Figure 15. Simulation results under the highway condition for the: a – flow rate requirement of the propulsion/working pump; b – power requirement of the propulsion/working system; c – command value of the engine speed; d – command value of the propulsion/working pump displacement; e – engine operating speed; f – engine operating torque

To respond to the requirement of Q_{PPadj} , V_{PPcmd} appears at a high level platform at 7 s. At 7...12 s, under the adaptive control of the propulsion pump based on pressure feedback, V_{PPcmd} is influenced by Q_{PPadj} (Figure 15a) and shows a remarkable valley value. Afterwards, V_{PPcmd} stabilizes, and its variation trend is also opposite to that of n_{Ecmd} .

The simulation results of the engine operating speed and torque are gained under the highway condition, as shown in Figures 15e and 15f, respectively, are presented as a scatter plot in the engine BSFC map, as shown in Figure 16.

As shown in Figure 16, under the highway condition and the proposed control, the simulation results of the engine operating speed and torque slightly fluctuate, and the ICE operating point is distributed near the vicinity of the ICE OOL of 15...25 kW and achieves the expected control effect.

3.2.4. Analysis of simulation results under the highway condition

The driver's operation and pressure data of the propulsion/working system under the off-road condition, as shown in Figure 12, are considered as the input of the COSIM platform. The simulation results are shown in Figure 17.

In Figure 17a, owing to the influence of the pressure fluctuation of propulsion system under the off-road condition (Figure 12b), the adjustment time of Q_{PPadj} by $k_{Q,PPadj}$ is significantly higher than that under the highway condition.

In Figures 17b–d, given the influence of the pressure fluctuation of the propulsion system under the off-road condition, the fluctuation amplitude of the simulation results of P_{Preq} , P_{req} , n_{Ecmd} , Q_{PPreq} and Q_{WPreq} is larger than that under the highway condition, but the variation trends and basic characteristics are similar.

The simulation results of the engine operating speed and torque are gained under the off-road condition, as shown in Figures 17e and 17f, respectively, are presented as a scatter plot in the engine BSFC map, as shown in Figure 18.

As shown in Figure 18, given the influence of the pressure fluctuation of the propulsion system under the off-road condition, compared with the highway condition, the fluctuation of the engine operating speed and torque is more intense, and the amplitude is larger. In the scatter plot of the ICE operating point, although its distribution is more disperse compared with the highway condition, it remains in the vicinity of the ICE OOL. This result shows that the control strategy proposed in this paper can also achieve the expected control effect under the off-road condition.

Conclusions

By referring to the power follower method of the hybrid EMS, this paper presented a new control strategy for the non-hybrid HST-CV with a traditional closed-loop HST

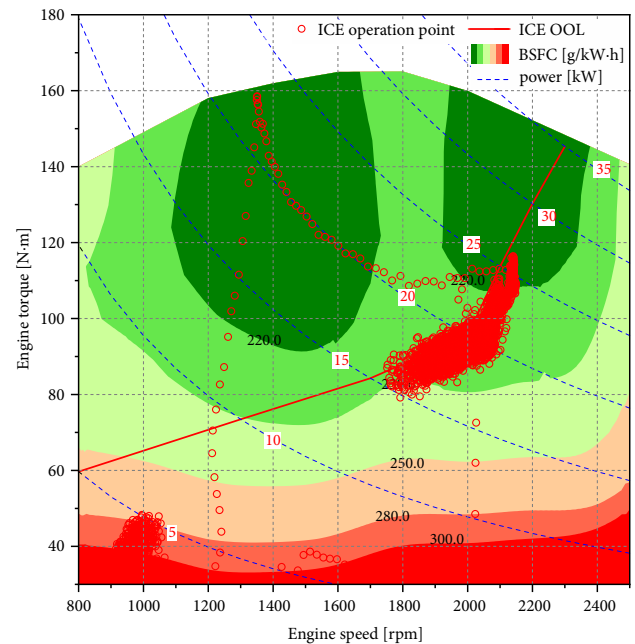


Figure 16. Scatter plot of the ICE operating point under the highway condition

for both the propulsion and working systems. The presented control method takes the flow rate of the HST-CV propulsion/working system as the control target. By coordinated control of the engine speed and hydraulic pump displacement, the decoupling between the engine speed and flow rate of the HST system can be achieved. Then, based on the overall power requirement of the HST-CV, the ICE operating point can be controlled at the desirable range of the engine. The proposed control strategy can achieve energy-saving control effects similar to the power follower control strategy of hybrid vehicles without installing additional accumulators in the HST system.

According to the structure principle and main parameters of the HST-CV basic vehicle, the layered control strategy structure was established and specific methods to implement the proposed control strategy were discussed. Then a MATLAB/SIMULINK–AMESIM COSIM platform was established to verify the control effect, and the input of the COSIM was obtained by the load data capturing experiment to ensure the accuracy of the simulation results. The simulation results show that the proposed control strategy can achieve the expected control target under both the highway and off-road conditions.

The proposed control strategy and corresponding results can be used as references for energy-saving transformations and the development of control systems, especially the application of advanced control strategies of CVs or road vehicles with a non-hybrid closed-loop HST system.

Acknowledgements

This work was supported by Program of State Key Laboratory of Smart Manufacturing for Special Vehicles and Transmission System (Grant No GZ2018KF004).

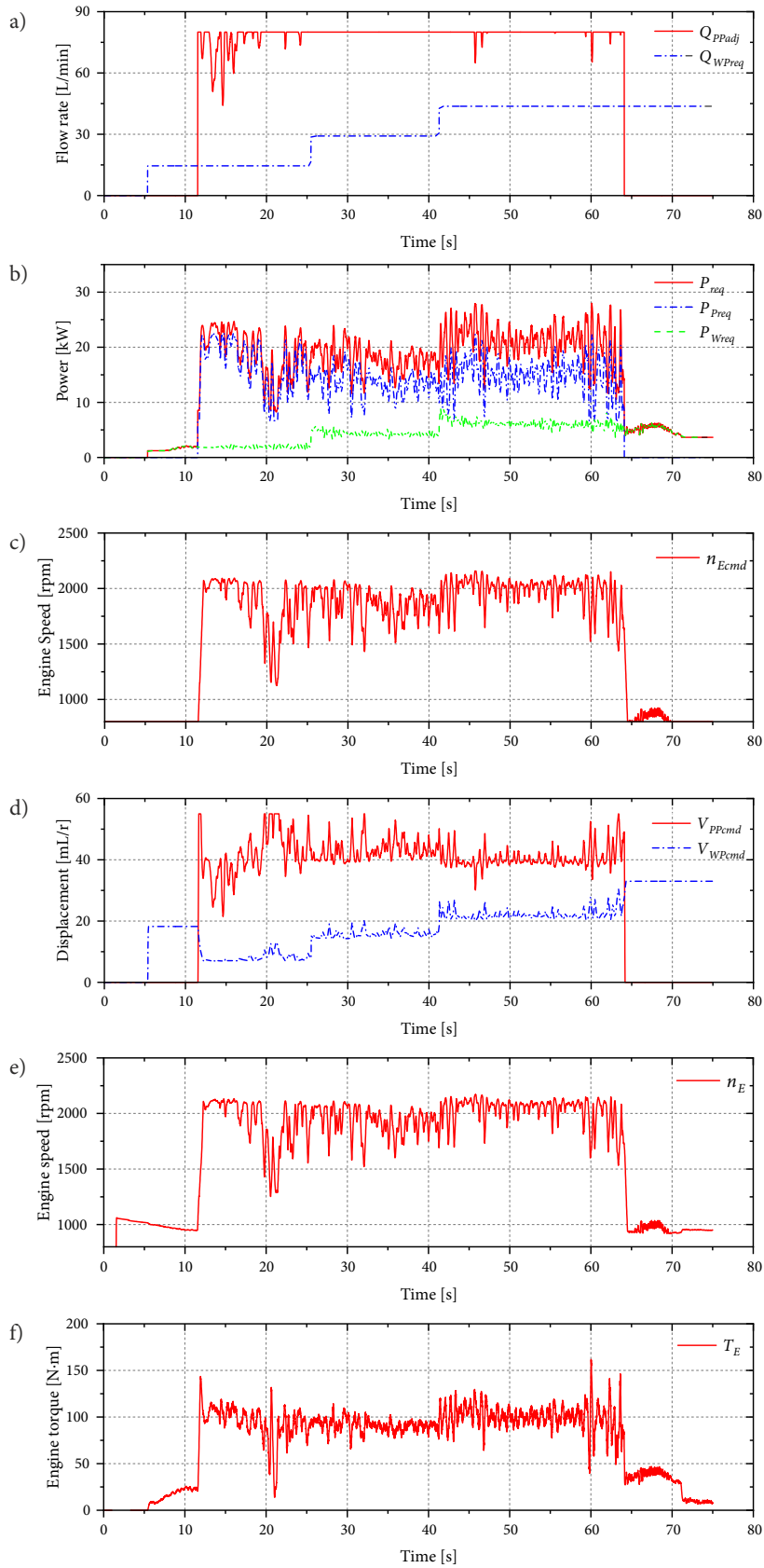


Figure 17. Simulation results under the off-road condition for the: a – flow rate requirement of the propulsion/working pump; b – power requirement of the propulsion/working system; c – command value of the engine speed; d – command value of the propulsion/working pump displacement; e – engine operating speed; f – engine operating torque

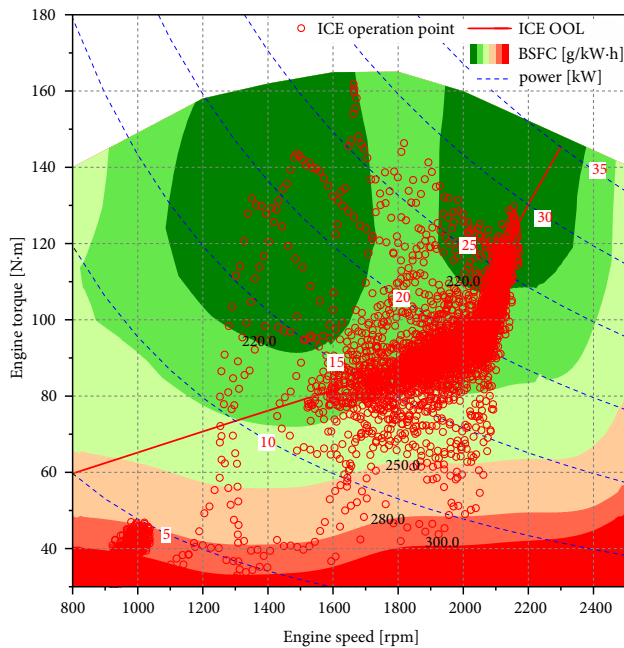


Figure 18. Scatter plot of ICE operating point under the off-road condition

Funding

This work was supported by the Program of State Key Laboratory of Smart Manufacturing for Special Vehicles and Transmission System (Grant No GZ2018KF004).

Author contributions

Haoyu Yuan and Yunwu Han conceived of the presented idea.

Haoyu Yuan, Yunwu Han, Shaofeng Du and Jindong Wang carried out the experiment.

Shaofeng Du contributed to measurement and interpretation of data, and Jindong Wang helped carry out the simulations.

Haoyu Yuan wrote the manuscript with support from Yunwu Han and Jixin Wang.

Jixin Wang supervised the project. Haoyu Yuan, Shaofeng Du, Yunwu Han, Jindong Wang critically reviewed the manuscript.

All authors approved the final version of the manuscript.

Disclosure statement

The authors have no financial conflicts of interest disclose concerning the study.

References

Aschemann, H.; Ritzke, J.; Schulte, H. 2009. Model-based non-linear trajectory control of a drive chain with hydrostatic transmission, *IFAC Proceedings Volumes* 42(13): 461–466. <https://doi.org/10.3182/20090819-3-PL-3002.00080>

- Backé, W. 1993. The present and future of fluid power, *Proceedings of the Institution of Mechanical Engineers, Part I: Journal of Systems and Control Engineering* 207(4): 193–212. https://doi.org/10.1243/PIME_PROC_1993_207_343_02
- Daikin-Sauer-Danfoss. 2020. *All Products Technical Information*. Daikin-Sauer-Danfoss Ltd. Available from Internet: <https://www.daikin-sauer-danfoss.com>
- Deppen, T. O.; Alleyne, A. G.; Meyer, J. I.; Stelson, K. A. 2015. Comparative study of energy management strategies for hydraulic hybrids, *Journal of Dynamic Systems, Measurement, and Control* 137(4): 041002. <https://doi.org/10.1115/1.4028525>
- Filipi, Z.; Kim, Y. J. 2010. Hydraulic hybrid propulsion for heavy vehicles: combining the simulation and engine-in-the-loop techniques to maximize the fuel economy and emission benefits, *Oil & Gas Science and Technology – Revue d'IFP Energies nouvelles* 65(1): 155–178. <https://doi.org/10.2516/ogst/2009024>
- GB20819-2014. *Limits and Measurement Methods for Exhaust Pollutants from Diesel Engines of Non-Road Mobile Machinery (China III, IV)*. National Standard of the People's Republic of China. Ministry of Ecology and Environment (MEE) the People's Republic of China. Available from Internet: <https://www.mee.gov.cn/ywgz/fgbz/bz/bzwb/dqjhbh/dqydywrwfbz/201405/W020140603336102800621.pdf> (in Chinese).
- Hung, C.-W.; Vu, T.-V.; Chen, C.-K. 2016. The development of an optimal control strategy for a series hydraulic hybrid vehicle, *Applied Sciences* 6(4): 93. <https://doi.org/10.3390/app6040093>
- Johri, R.; Filipi, Z. 2014. Optimal energy management of a series hybrid vehicle with combined fuel economy and low-emission objectives, *Proceedings of the Institution of Mechanical Engineers, Part D: Journal of Automobile Engineering* 228(12): 1424–1439. <https://doi.org/10.1177/0954407014522444>
- Kim, M.; Jung, D.; Min, K. 2014. Hybrid thermostat strategy for enhancing fuel economy of series hybrid intracity bus, *IEEE Transactions on Vehicular Technology* 63(8): 3569–3579. <https://doi.org/10.1109/TVT.2013.2290700>
- Kim, Y.; Filipi, Z. 2007. Series hydraulic hybrid propulsion for a light truck – optimizing the thermodynamic power management, *SAE Technical Paper* 2007-24-0080. <https://doi.org/10.4271/2007-24-0080>
- Korn, J. 1969. *Hydrostatic Transmission Systems*. TBS The Book Service Ltd. 355 p.
- Li, T.; Liu, H.; Zhao, D.; Wang, L. 2016. Design and analysis of a fuel cell supercapacitor hybrid construction vehicle, *International Journal of Hydrogen Energy* 41(28): 12307–12319. <https://doi.org/10.1016/j.ijhydene.2016.05.040>
- Mishra, R.; Saad, S. M. 2017. Simulation based study on improving the transient response quality of turbocharged diesel engines, *Journal of Quality in Maintenance Engineering* 23(3): 297–309. <https://doi.org/10.1108/JQME-08-2016-0037>
- Molla, S. 2010. *System Modeling and Power Management Strategy for a Series Hydraulic Hybrid Vehicle*. MSc Thesis. Clemson University, Clemson, SC, US. 121 p. Available from Internet: https://tigerprints.clemson.edu/all_theses/844
- Nawrocka, A.; Kwaśniewski, J. 2008. Predictive neural network controller for hydrostatic transmission control, *Mechanics* 27(2): 62–65. Available from Internet: <https://journals.bg.agh.edu.pl/MECHANICS/2008-02/mech03.pdf>
- Rydberg, K. 1998. Hydrostatic drives in heavy mobile machinery – new concepts and development trends, *SAE Technical Paper* 981989. <https://doi.org/10.4271/981989>
- Schumacher, A.; Rahmfeld, R.; Laffrenzen, H. 2016. High Performance Drivetrains for Powerful Mobile Machines, in 10th

- International Fluid Power Conference (10. IFK), 8–10 March 2016 Dresden, Germany, 3: 53–68. Available from Internet: <https://tud.qucosa.de/api/qucosa%3A29380/attachment/ATT-0/>
- Shabbir, W.; Evangelou, S. A. 2016. Exclusive operation strategy for the supervisory control of series hybrid electric vehicles, *IEEE Transactions on Control Systems Technology* 24(6): 2190–2198. <https://doi.org/10.1109/TCST.2016.2520904>
- Sun, H.; Aschemann, H. 2013. Sliding-mode control of a hydrostatic drive train with uncertain actuator dynamics, in *2013 European Control Conference (ECC)*, 17–19 July 2013, Zurich, Switzerland, 3216–3221. <https://doi.org/10.23919/ECC.2013.6669571>
- Vu, T.-V.; Chen, C.-K.; Hung, C.-W. 2014. A model predictive control approach for fuel economy improvement of a series hydraulic hybrid vehicle, *Energies* 7(11): 7017–7040. <https://doi.org/10.3390/en7117017>
- Wu, K.; Zhang, Q.; Hansen, A. 2004. Modelling and identification of a hydrostatic transmission hardware-in-the-loop simulator, *International Journal of Vehicle Design* 34(1): 52–64. <https://doi.org/10.1504/IJVD.2004.003894>
- Zhao, L.; Wang, J.; Zhang Z. 2018. Research on vehicle speed control strategy of multi-axis hydrostatic transmission, in *Proceedings of the 2018 3rd International Workshop on Materials Engineering and Computer Sciences (IWMECS 2018)*, 27–28 January 2018, Jinan, China, 410–415. <https://doi.org/10.2991/iwmecs-18.2018.88>
- Zips, P.; Lobe, A.; Trachte, A.; Kugi, A. 2019. Torque control of a hydrostatic transmission applied to a wheel loader, in *2019 IEEE 58th Conference on Decision and Control (CDC)*, 11–13 December 2019, Nice, France, 4273–4279. <https://doi.org/10.1109/CDC40024.2019.9030128>